



A fluorescent sensor for pH based on rhodamine fluorophore

Maozhong Tian^{a,b}, Xiaojun Peng^a, Jiangli Fan^{a,*}, Jingyun Wang^a, Shiguo Sun^a

^a State Key Laboratory of Fine Chemicals, Dalian University of Technology, 2 Linggong Rd., Hi-tech Zone, Dalian 116024, People's Republic of China

^b College of Chemistry and Chemistry Engineering, Shanxi Datong University, Datong 037009, People's Republic of China

ARTICLE INFO

Article history:

Received 26 December 2011

Received in revised form

3 March 2012

Accepted 8 March 2012

Available online 28 March 2012

Keywords:

Fluorescence

Sensor

pH

Rhodamine

Selectivity

Acidic

ABSTRACT

In this study, an 'Off–On'-type acidic pH fluorescent chemosensor, 3',6'-Bis (ethylamino)-2',7'-dimethyl-2-(2-oxoethylideneamino)spiro[isindoline-1,9'-xanthen]-3-one (**RG1**) has been designed, synthesized, and characterized by high-resolution mass spectrometry (HRMS), X-ray crystallography, infrared spectroscopy (IR), and ¹H NMR and ¹³C NMR spectroscopy. The design tactics for the sensor was based on the change in structure between spirocyclic (non-fluorescent) and ring-open (fluorescent) forms of rhodamine dyes. Fluorescence "off–on" behaviors of **RG1** were investigated on the basis of variable acid concentrations. The pH titrations showed a ca. 581-fold increase in fluorescence intensity within the pH range of 7.5 to 1.1 with a pK_a value of 2.32 in acetonitrile–water (1:1, v/v) solution when excited at 510 nm. The fluorescence change of **RG1** was fully reversible and took place mainly within the pH range from 1.0 to 4.0, which was valuable for pH researches in acidic environments.

Crown Copyright © 2012 Published by Elsevier Ltd. All rights reserved.

1. Introduction

The detection of pH is critical important because it usually plays a pivotal role in a variety of systems. The most common pH sensors are glass electrodes. However, the known limitations of the glass pH electrodes (e.g., its electrical interference or mechanical destruction to small cells) make them unsuitable for certain applications: intracellular pH and microscopy studies. In contrast to the electrochemical methods, optical measurements based on fluorescent probes have no such faults [1,2]. Moreover, fluorescent probes have their obvious advantages in terms of sensitivity, selectivity, subnanometer spatial resolution, more convenient operation in many applications (e.g., remote sensing with fiber optics) [3–10].

Several fluorescence pH sensors have been reported in the literature [11–26]. To the best of our knowledge, however, relatively less attention was paid on the fluorescent probes which are pH sensitive in the lower pH region (pH < 4). In fact, since some media such as those found in the human stomach or environmental water are strongly acidic, it is necessary to develop chemosensors for monitoring pH level of these strongly acidic media.

The rhodamine derivatives used as fluorescent probes [27–31] have received a great deal of attention from organic chemists because of its excellent photophysical properties, such as long absorption and emission wavelengths elongated to the visible region, high fluorescence quantum yield, and large absorption coefficient. Herein, we designed and synthesized sensor **RG1** based on rhodamine 6G. The fluorescence change of the sensor took place mainly within the pH range from 1.0 to 4.0. The sensor was characterized by HRMS, IR, X-ray crystallography, ¹H NMR and ¹³C NMR. The mechanism of the sensor to monitor H⁺ is based on the change in structure between spirocyclic and open-cycle forms. Without H⁺, the sensor exists in a spirocyclic form, which is colorless and non-fluorescent. Addition of H⁺ leads to a spirocycle open, resulting in an appearance of pink color and fluorescence.

2. Experimental part

2.1. Materials and apparatus

Acetonitrile and deionized water were used as solvents. All the materials for synthesis were purchased from commercial suppliers and used without further purification. With the exception of HgCl₂, aqueous solutions of metal ions were prepared from their nitrate salts. Flash chromatography was carried out on silica gel SG1105 (200–300 mesh; Qingdao Makall).

* Corresponding author. Tel.: +86 411 84986327; fax: +86 411 84983606.

E-mail address: fanjl@dlut.edu.cn (J. Fan).

^1H NMR and ^{13}C NMR spectra were recorded on a Varian INVOA 400 MHz spectrometer. Chemical shifts (δ) were reported in ppm relative to a Me_4Si standard in CDCl_3 and coupling constants (J) in Hz. Mass spectra were obtained using a Q-TOF mass spectrometry (Micromass, England). Absorption spectra were obtained on a Perkin Elmer Lambda 35 UV/Vis spectrophotometer at 298 ± 1 K. Steady-state fluorescence spectra were measured using a 10 mm path length quartz cell on a Perkin Elmer LS55 fluorescence spectrophotometer at 298 ± 1 K. A Model pH5-3C digital pH meter (Shanghai, China) was employed to make the pH measurements. Data of the single crystals were collected on a Bruker SMART CCD diffractometer at 293 K. IR spectra were recorded on a Nicolet Nexus 770 spectrometer.

2.2. Synthesis of compound RG1

The synthetic route of **RG1** is shown in Scheme 1. Rhodamine 6G hydrazide (compound **1**) was synthesized according to the literature [29]. Compound **1** (0.30 g, 0.7 mmol) was dissolved in 15 ml of absolute ethanol. Excess oxalaldehyde hydrate (2.0 ml; oxalaldehyde content >40 mass%) was added, then the mixture was stirred under N_2 atmosphere for 8 h. The solvent was removed under reduced pressure. The crude product was purified by flash column chromatography on silica gel with EtOAc/petroleum spirit (1/6, v/v) as eluent, affording 217.0 mg of compound **RG1** as a yellow solid (yield 66.2%). HRMS (ESI) m/z : calcd for $\text{C}_{28}\text{H}_{32}\text{N}_4\text{O}_3$ [$\text{M} + \text{H}$] $^+$ 469.2240; found 469.2229. ^1H NMR (400 MHz, CDCl_3): δ (ppm) = 9.23 (d, $J = 7.6$ Hz, 1H), 7.98 (d, $J = 7.2$ Hz, 1H), 7.63–7.55 (m, 2H), 7.44 (d, $J = 7.6$ Hz, 1H), 7.02 (d, $J = 7.6$ Hz, 1H), 6.34 (s, 2H), 6.28 (s, 2H), 4.17 (s, 2H), 3.22–3.16 (m, 4H), 1.85 (s, 6H), 1.26 (t, $J = 6.8$ Hz, 6H); ^{13}C NMR (100 MHz, CDCl_3): δ (ppm) = 191.97, 153.85, 151.27, 148.69, 140.91, 135.39, 129.17, 128.27, 127.21, 123.05, 119.21, 118.87, 104.22, 102.76, 96.17, 72.90, 64.58, 38.08, 33.05, 16.10, 14.83, 13.84. IR (KBr, cm^{-1}): 3381, 2968, 2925, 2870, 1669, 1635, 1615, 1548, 1517, 1467, 1357, 1309, 1266, 1221, 1122, 824, 785, 762, 702.

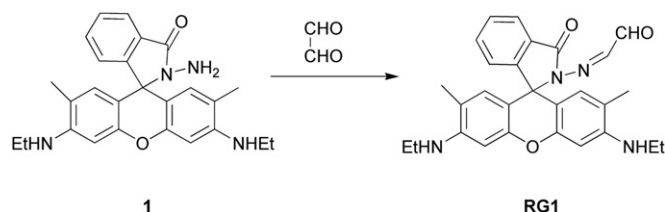
2.3. Crystal growth

The quality of single crystals depends on the purity of the used material. Hence, the synthesized material was highly purified material. The saturated hexane–dichloromethane (5:1, v/v) solution was prepared at room temperature (25 °C). Then, the prepared solution was filtered into a beaker and covered to restrict the fast evaporation of the solvent. Finally, the prepared solution was kept in a constant temperature (25 °C). After a span of about 20 days, yellow single crystals of compound **RG1** were obtained.

3. Results and discussion

3.1. Single crystal X-ray structure analysis

X-ray crystallography structural investigation of **RG1** revealed that the main skeleton of the molecule is formed from a xanthene ring and a spirolactam ring. The xanthene ring is close to planar



Scheme 1. The synthetic route of sensor **RG1**.

Table 1

The crystallographic data and structure refinement parameters of **RG1**.

Empirical formula	$\text{C}_{28}\text{H}_{32}\text{N}_4\text{O}_3$
Formula weight	468.55
Temperature	298 (2) K
Wavelength	0.71073
Crystal system, Space group	Orthorhombic, Pna2(1)
Unit cell dimensions	$a = 19.3581(16)$ Å, $\alpha = 90.00^\circ(10)$ $b = 8.3951(5)$ Å, $\beta = 90.00^\circ(5)$ $c = 15.7549(13)$ Å, $\gamma = 90.00^\circ(6)$
Volume	$2560.4(3)$ Å ³
Z	4
Density (calculated)	1.218 Mg m ⁻³
Absorption coefficient	0.081 mm ⁻¹
$F(0\ 0\ 0)$	996
Crystal size	0.38 mm \times 0.10 mm \times 0.10 mm
Theta range for data collection	2.47 – 27.49°
Limiting indices	$-25 \leq h \leq 23$, $-10 \leq k \leq 10$, $-17 \leq l \leq 20$
Absorption correction	Multi-scan
Refinement method	Full-matrix least-squares on F^2
Data/restraints/parameters	4739/1/340
Goodness-of-fit on F^2	1.02
Final R indices [$I > 2\sigma(I)$]	$R1 = 0.1135$, $wR = 0.1500$
R indices (all data)	$R1 = 0.0498$, $wR = 0.1154$

with an r.m.s. deviation of $0.135(1)$ Å. The lactam moiety of the molecule is oriented nearly orthogonal to the xanthene moiety. The dihedral angle between the planes of the xanthene and the spirolactam rings systems is $90.4(1)^\circ$. The crystallographic data and structure refinement parameters of **RG1** are presented in Table 1. The thermal ellipsoid plot using ORTEP3 drawn at 30% probability level of the molecule of **RG1** along with the atom numbering scheme is shown in Fig. 1.

3.2. Influence of protons on the absorbance and fluorescence intensity

RG1 exhibits very weak absorption in the pH 5.0–13.2 range in an acetonitrile–water (1:1, v/v) solution. It can be explained that **RG1** exists in the form of spirocyclic structure in the solution. As the pH (<5) decreases, the absorption band at 532 nm was observed to increase distinctly (Fig. 2). Meanwhile, the colorless solution of **RG1** rapidly turned into pink due to the ring-opening process by **RG1** interacting with protons. Subsequent addition of NaOH resulted in

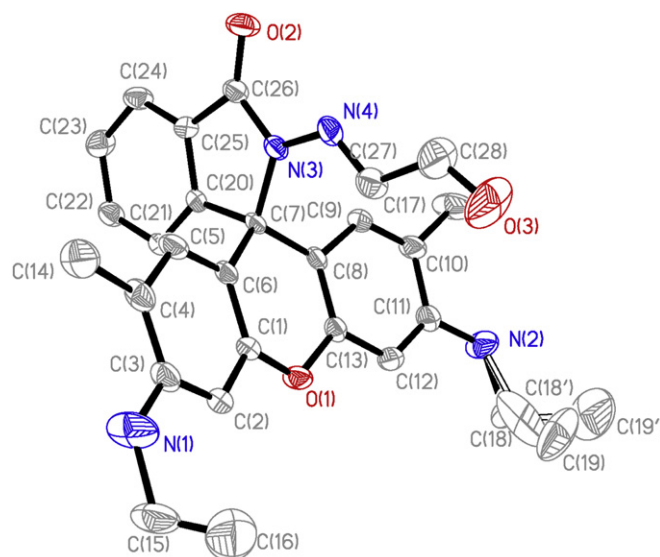


Fig. 1. Thermal ellipsoid plot using ORTEP3 drawn at 30% probability level of the molecule of **RG1** along with the atom numbering scheme.

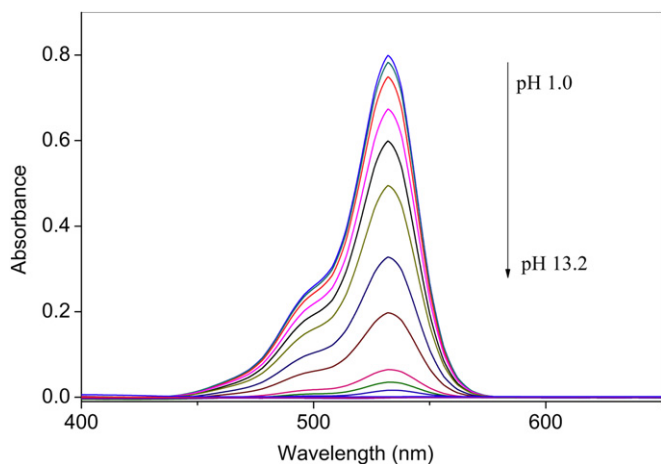


Fig. 2. Dependence of absorption spectra of **RG1** (20 μ M) on pH 13.2–1.0 in acetonitrile–water (1:1, v/v) solution.

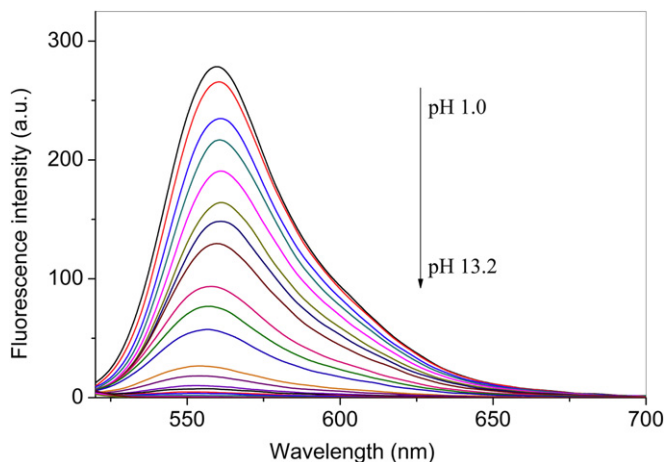


Fig. 3. Dependence of fluorescent spectra of **RG1** (20 μ M) on pH 13.2–1.0 in acetonitrile–water (1:1, v/v) solution. Excitation was at 510 nm.

colorless solution, implying a reversible coordination process between **RG1** and H^+ . Both the color and spectra changes indicate that **RG1** can probe pH reversibly and this detection process can be easily observed by naked eyes.

On the other hand, the emission spectra of **RG1** at different pH values in an acetonitrile–water (1:1, v/v) solution are shown in Fig. 3. Only very weak emission was observed in alkaline solution between 350 nm and 650 nm. However, with a decrease in pH, the fluorescence intensities of **RG1** gradually increased with a 28 nm bathochromic shift from 532 nm to 560 nm. The fluorescence intensity in low pH (1.1) was ca. 581-fold larger than that in high pH

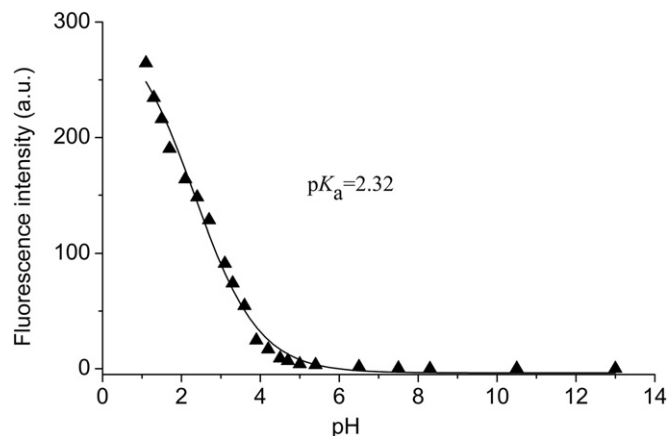


Fig. 4. Fluorescent intensity (560 nm) of **RG1** (20 μ M) versus pH in acetonitrile–water (1:1, v/v) solution. Excitation was at 510 nm.

(7.5) for probe **RG1**. The fluorescence change of the probe **RG1** was also fully reversible and took place mainly within the pH range from 1.0 to 4.0. This fluorescence enhancement in low pH is due to the ring-opening of **RG1** by protons (Scheme 2).

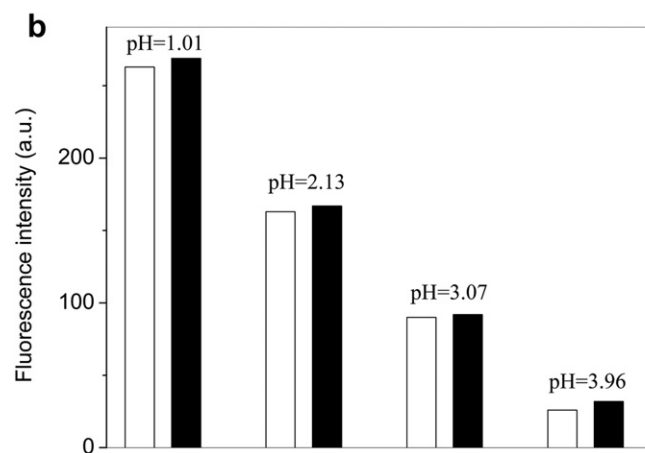
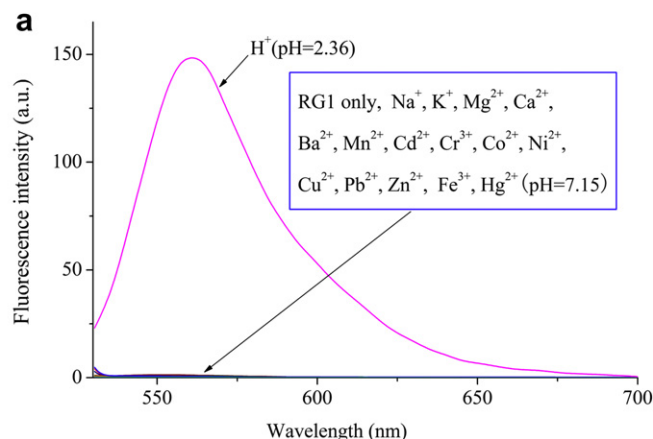
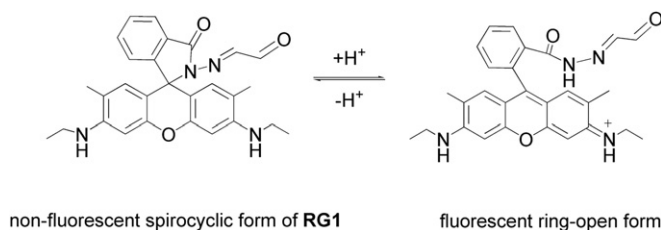


Fig. 5. Fluorescence responses of **RG1** in the presence of different metal ions and proton. (a) Influence of different metal ions (200 μ M) and proton on the fluorescent spectra of **RG1** (20 μ M) in $CH_3CN/Tris-HCl$ buffer (1:1, v/v, pH 7.15). (b) Fluorescence maxima of **RG1** at different pH (in CH_3CN/H_2O solution for pH 1.01, in $CH_3CN/Britton-Robinson$ buffer for pH 2.13, 3.07 and 3.96). White column: without extraneous metal ions; black column: with Na^+ , K^+ (10 mM), Mg^{2+} , Ca^{2+} (5 mM), Ba^{2+} , Mn^{2+} , Cd^{2+} , Cr^{3+} , Co^{2+} , Ni^{2+} , Cu^{2+} , Pb^{2+} , Zn^{2+} , Fe^{3+} , Hg^{2+} (200 μ M). λ_{ex} = 510 nm and λ_{em} = 560 nm.



Scheme 2. Proposed mechanism for the fluorescence enhancement of **RG1** upon the addition of H^+ .

The acidity constants K_a of **RG1** was determined in acetonitrile/water (1:1, v/v) solution by fluorimetric titration as a function of pH (Fig. 4). Sigmoidal curve fitting of Henderson–Hasselbach-type mass action equation (1) [32,33] to the fluorescence intensity I recorded as a function of pH yielded values of pK_a , where I is the observed fluorescence intensity at a fixed wavelength, I_{\max} and I_{\min} are the corresponding maximum and minimum, respectively. We got a pK_a of 2.32 (± 0.16), which is valuable for studying the strong acid pH scale.

$$pK_a = \text{pH} - \log \frac{I_{\max} - I}{I - I_{\min}} \quad (1)$$

3.3. Selectivity for H^+

Considering that nitrogen and oxygen can bind many metal ions in solution, it is very important to determine whether other ions are potential interferents. Upon addition of Na^+ , K^+ , Mg^{2+} , Ca^{2+} , Ba^{2+} , Mn^{2+} , Cd^{2+} , Cr^{3+} , Co^{2+} , Ni^{2+} , Cu^{2+} , Pb^{2+} , Zn^{2+} , Fe^{3+} and Hg^{2+} to the 20 μM **RG1** solutions while keeping the other experimental condition unchanged at pH 7.15, no significant fluorescence intensity changes were observed (Fig. 5a). It is probably because there are not sufficient coordination sites between various metal ions and **RG1**, which cannot induce the spirolactam ring-open and emit fluorescence of rhodamine 6G. However, a certain amount of H^+ led to a remarkable enhancement in fluorescence intensity. Furthermore, the fluorescence intensity changes caused by H^+ are not significantly influenced by the coexisting metal ions at pH 1.01, 2.13, 3.07, and 3.96 (Fig. 5b). The results indicate that **RG1** can selectively measure pH changes in the presence of various metal ions.

4. Conclusion

In this work, a fluorescent pH sensor (**RG1**) based on rhodamine fluorophore has been synthesized, and its photophysical behavior was examined as a function of pH. In aqueous solution, **RG1** showed a large fluorescent enhancement upon increasing the acidity of the solution. It can be used in aqueous solution as fluorescent pH sensors excitable with visible light. Metal ions including Na^+ , K^+ , Mg^{2+} , Ca^{2+} , Ba^{2+} , Mn^{2+} , Cd^{2+} , Cr^{3+} , Co^{2+} , Ni^{2+} , Cu^{2+} , Pb^{2+} , Zn^{2+} , Fe^{3+} , Hg^{2+} had no significant interference on pH determination. The enhancement of color and fluorescence in acidic solutions was in the range of 450–650 nm, thus, the compound was able to serve as a “naked-eye” chemosensor for pH. The fluorescence change of **RG1** was fully reversible and took place mainly within the pH range from 1.0 to 4.0. Therefore, we expect that this fluorescent sensor would be able to monitor pH levels in a human stomach or some acidic environments.

Acknowledgments

This work was supported by NSF of China (21136002, 21076032, 21072024 and 20923006), National Basic Research Program of China (2009CB724706), Scientific Research Fund of Liaoning Provincial Education Department (LS2010040), and the Shanxi Scholarship Council of China (No. 20090980).

References

- [1] Ogikubo S, Nakabayashi T, Adachi T, Islam MS, Yoshizawa T, Kinjo M, et al. Intracellular pH sensing using autofluorescence lifetime microscopy. *J Phys Chem B* 2011;115(34):10385–90.
- [2] Zhang WS, Tang B, Liu X, Liu YY, Xu KH, Ma JP, et al. A highly sensitive acidic pH fluorescent probe and its application to HepG2 cells. *Analyst* 2009;134(2):367–71.
- [3] de Silva AP, Gunaratne HQN, Gunlaugsson T, Huxley AJM, McCoy CP, Rademacher JT, et al. Signaling recognition events with fluorescent sensors and switches. *Chem Rev* 1997;97(5):1515–66.
- [4] Martínez-Máñez R, Sancenón F. Fluorogenic and chromogenic chemosensors and reagents for anions. *Chem Rev* 2003;103(11):4419–76.
- [5] Swamy KMK, Ko S, Kwon SK, Lee HN, Mao C, Kim J, et al. Boronic acid-linked fluorescent and colorimetric probes for copper ions. *Chem Commun* 2008;45:5915–7.
- [6] Du JJ, Fan JL, Peng XJ, Sun PP, Wang JY, Li HL, et al. A new fluorescent chemodosimeter for Hg^{2+} : selectivity, sensitivity, and resistance to Cys and GSH. *Org Lett* 2010;12(3):476–9.
- [7] Zhang LZ, Wang JY, Guo KX, Peng XJ. A highly selective, fluorescent chemosensor for bioimaging of Fe^{3+} . *Bioorg Med Chem Lett* 2011;21(18):5413–6.
- [8] Du PW, Lippard SJ. A highly selective turn-on colorimetric, red fluorescent sensor for detecting mobile zinc in living cells. *Inorg Chem* 2010;49(23):10753–5.
- [9] Niu CG, Gui XQ, Zeng GM, Guan AL, Gao PF, Qin PZ. Fluorescence ratiometric pH sensor prepared from covalently immobilized porphyrin and benzo-thioxanthene. *Anal Bioanal Chem* 2005;383:349–57.
- [10] Kim HN, Guo ZQ, Zhu WH, Yoon J, Tian H. Recent progress on polymer-based fluorescent and colorimetric chemosensors. *Chem Soc Rev* 2011;40(1):79–93.
- [11] Baruah M, Qin WW, Basarić N, Borggraefe WMD, Boens N. BODIPY-based hydroxyaryl derivatives as fluorescent pH probes. *J Org Chem* 2005;70(10):4152–7.
- [12] Bergen A, Granzhan A, Ihmels H. Water-soluble, pH-sensitive fluorescent probes on the basis of acridizinium ions. *Photochem Photobiol Sci* 2008;7(4):405–7.
- [13] Tian MZ, Peng XJ, Feng F, Meng SM, Fan JL, Sun SG. Fluorescent pH probes based on boron dipyrromethene dyes. *Dyes Pigm* 2009;81(1):58–62.
- [14] Murtagh J, Frimannsson DO, O'Shea DF. Azide conjugatable and pH responsive near-infrared fluorescent imaging probes. *Org Lett* 2009;11(23):5386–9.
- [15] Tang B, Yu FB, Li P, Tong LL, Duan X, Xie T, et al. A near-infrared neutral pH fluorescent probe for monitoring minor pH changes: imaging in living HepG2 and HL-7702 cells. *J Am Chem Soc* 2009;131(8):3016–23.
- [16] Xiao HB, Li H, Chen MJ, Wang L. A water-soluble D- π -A chromophore based on dipicolinic acid: synthesis, pH-dependent spectral properties and two-photon fluorescence cell imaging. *Dyes Pigm* 2009;83(3):334–8.
- [17] Lu HG, Xu B, Dong YJ, Chen FP, Li YW, Li ZF, et al. Novel fluorescent pH sensors and a biological probe based on anthracene derivatives with aggregation-induced emission characteristics. *Langmuir* 2010;26(9):6838–44.
- [18] Jäger WF, Hammink TS, Berg OVD, Grozema FC. Highly sensitive water-soluble fluorescent pH sensors based on the 7-amino-1-methylquinolinium chromophore. *J Org Chem* 2010;75(7):2169–78.
- [19] Liu ZP, Zhang CL, He WJ, Qian F, Yang XL, Gao X, et al. A charge transfer type pH responsive fluorescent probe and its intracellular application. *New J Chem* 2010;34(4):656–60.
- [20] Shen LJ, Lu XY, Tian H, Zhu WH. A long wavelength fluorescent hydrophilic copolymer based on naphthalenediimide as pH sensor with broad linear response range. *Macromolecules* 2011;44(14):5612–8.
- [21] Boens N, Qin WW, Baruah M, De Borggraefe WM, Filarowski A, Smidom N, et al. Rational design, synthesis, and spectroscopic and photophysical properties of a visible-light-excitable, ratiometric, fluorescent near-neutral pH indicator based on BODIPY. *Chem – Eur J* 2011;17(39):10924–34.
- [22] Wan XJ, Liu SY. Fluorescent water-soluble responsive polymers site-specifically labeled with FRET dyes possessing pH- and thermo-modulated multicolor fluorescence emissions as dual ratiometric probes. *J Mater Chem* 2011;21(28):10321–9.
- [23] Lee H, Akers W, Bhushan K, Bloch S, Sudlow G, Tang R, et al. Near-infrared pH-activatable fluorescent probes for imaging primary and metastatic breast tumors. *Bioconjug Chem* 2011;22(4):777–84.
- [24] Ju CC, Yin HJ, Yuan CL, Wang KZ. A fluorescent probe for both pH and Zn^{2+} based on 2-(1-phenyl-1H-benzod[imidazol-2-yl])phenol. *Spectrochim Acta Part A* 2011;79(5):1876–80.
- [25] Best QA, Xu RS, McCarroll ME, Wang LC, Dyer DJ. Design and investigation of a series of rhodamine-based fluorescent probes for optical measurements of pH. *Org Lett* 2010;12(14):3219–21.
- [26] Li Z, Wu SQ, Han JH, Han SF. Imaging of intracellular acidic compartments with a sensitive rhodamine based fluorogenic pH sensor. *Analyst* 2011;136:3698–706.
- [27] Kim HN, Lee MH, Kim HJ, Kim JS, Yoon J. A new trend in rhodamine-based chemosensors: application of spirolactam ring-opening to sensing ions. *Chem Soc Rev* 2008;37(8):1465–72.
- [28] Beija M, Afonso CAM, Martinho JMG. Synthesis and applications of rhodamine derivatives as fluorescent probes. *Chem Soc Rev* 2009;38(8):2410–33.
- [29] Ko SK, Yang YK, Tae J, Shin I. In vivo monitoring of mercury ions using a rhodamine-based molecular probe. *J Am Chem Soc* 2006;128(43):14150–5.
- [30] Chen XQ, Pradhan T, Wang F, Kim JS, Yoon J. Fluorescent chemosensors based on spiroring-opening of xanthenes and related derivatives. *Chem Rev* 2011. ASAP.
- [31] Li HL, Fan JL, Wang JY, Tian MZ, Du JJ, Sun SG, et al. A fluorescent chemodosimeter specific for cysteine: effective discrimination of cysteine from homocysteine. *Chem Commun* 2009;39:5904–6.
- [32] Henderson LJ. Concerning the relationship between the strength of acids and their capacity to preserve neutrality. *Am J Physiol* 1908;21:173–9.
- [33] Valeur B. Molecular fluorescence: principles and applications. New York: Wiley-VCH Verlag GmbH; 2001. p. 276–8.